Journal of Solar Energy Research (JSER)

Journal homepage: www.jser.ut.ac.ir

Thermodynamic Analysis of ORC-GT Hybrid Cycle and Thermal Recovery from Photovoltaic Panels

Somayeh Davoodabadi Farahani[a,*], Mohammad Borzabadi Farahani[a], Ali Sajedi[a]

[a]School of Mechanical Engineering, Arak University of Technology, 38181-41167, Arak, Iran

Received: 07-06-2021
Accepted: 01-11-2022

Abstract

Biomass and solar energy are considered attractive renewable energy sources for power generation plants. In this research, the thermodynamic analysis of the organic Rankine cycle (ORC)-gas turbine-photovoltaic panel (PV) is investigated. Biogas is used as a heat source in the gas turbine cycle. Photovoltaic panel is also used for heating the combustion air. In a gas turbine cycle, the passing air passes through a photovoltaic system and heats up before entering the combustion chamber. Biogas, 60% methane and 40% carbon dioxide, is used as fuel in gas turbines. Sensitivity analysis was performed for cycle input variables. Results display that the output power of the modified cycle is increased by about 28% compared to the base cycle. The use of photovoltaic panel increases the power of the cycle by 23%-25%. The results of the analysis of the second law of thermodynamics show that the most exergy destruction belongs to the combustion chamber. The use of a photovoltaic panel reduces the amount of exergy destruction in the combustion chamber. Increasing condenser pressure and steam turbine pressure reduces power cycle energy efficiency. The lowest and highest exergy efficiencies are related to condenser and gas turbine, respectively. Findings display that the overall cost of the proposed cycles increases with the increase of the compressor pressure ratio and the temperature of the inlet fluid to the turbine.

Keywords: Photovoltaic panel; Biogas; Gas turbine; Organic Rankine cycle; Thermodynamic analysis

DOI: 10.22059/jser.2022.325213.1206 DOR: 20.1001.1.25883097.2022.7.4.6.1

1. Introduction

Today, the issue of energy supply from renewable source has become a basic need and many countries are looking for renewable sources to produce energy due to depletion of fossil fuel resources. Geothermal energy is a renewable method that has a high economic capacity to generate electrical power [1, 2]. Although high-temperature geothermal sources are more economical, but because most geothermal sources are in the low temperature range, it is predicted that the next generation of geothermal power plants will use more low-temperature sources [3]. Organic Rankine Cycle (ORC) is a power generation cycle that can be started using low temperature energy sources due to the use of low fluid boiling point organic fluids [4].

Hydrogen is considered as a carrier of clean energy for the production of environmentally friendly energy, which is mainly used in the power plant and chemical industries [5, 6]. In addition, it can be

*Corresponding Author Email Address: Sdfarahani@arakut.ac.ir

effectively converted to electricity in fuel cell systems with negligible greenhouse effects [7,8]. Today, hydrogen can be produced through fossil fuel sources, hydrocarbon reforming processes, and water electrolysis, but due to limited resources. Fossil as well as changes in climatic conditions due to the emission of carbon dioxide and other pollutants, the use of renewable and clean energy sources have been considered [9]. Meanwhile, water electrolysis is an accepted technology for large-scale hydrogen production. Hydrogen production by electrolysis through a proton membrane exchanger (PEM) has many advantages, including very low environmental effects and easy maintenance [10].

Simultaneous production is one of the best ways to conserve and store energy, which allows the efficient use of energy resources and help to preserve the environment. Simultaneous production enables the production of electricity and other useful types of energy (heat, cold, hot water, fresh water, hydrogen, etc.) from a single source [11]. Among different energy sources, geothermal energy has significant potential for hydrogen production. All or part of the output power of a geothermal power plant can be used to produce hydrogen through the water electrolysis process. It seems that hydrogen production based on geothermal energy and by water electrolysis operation will have an undeniable role in the economy of hydrogen production [12]. There is a lot of research on the use of a geothermal source to produce hydrogen [13-15].

However, it should be noted that exhaust gases from turbine are among the unused heat sources for use in the organic Rankine cycle. Also, the use of thermal photovoltaic panels to increase the inlet temperature to the combustion chamber is one of the solutions to improve the exergy and thermal efficiency of the organic Rankine cycle. Researchers have done a great deal of research in this area, including the work of Quolin et al. [16] on the economic and thermodynamic optimization of a small-scale ORC cycle for heat recovery. Deepak et al. [17] developed energy and exergy analysis for an improved organic Rankine cycle, showing that the efficiency of the first law is generally improved by using this cycle. Tchanche et al. [18] found that the natural state and temperature of hot springs significantly affect the organic fluid selection of the organic Rankine cycle.

Khaljani et al. [19] also analysed the co-production cycle of heat and power from the point of view of exergy and exergy-economy. In this work, they showed that the combustion chamber is the largest exergy destroyer of such systems.

Astolfi et al. [20] examined a combined concentrating solar power system and a geothermal binary plant based on an organic Rankine cycle. They designed a supercritical ORC for the optimal utilization of an intermediate enthalpy geothermal source. The plant also included a solar parabolic trough field, introducing an additional high temperature heat source for the cycle and increasing power production. They performed a differential economic analysis to determine the cost of the additional electricity generated by the solar source. There are other similar works that have obtained similar results [21]. Hezavei et al. [22] investigated different heat sources on the efficiency and cost of organic Rankine cycle. They found that the use of gas microturbines and solar energy increases the cost of the cycle. Sohbatloo and Boyaghchi [23] explored a cascade organic Rankine cycle with the solar collector and LNG. Ouagued [24] analysed an integrated Magnesium-Chlorine Mg-Cl thermochemical cycle with solar parabolic trough system. Gharibshahian et al. [25] evaluated a grid connected solar photovoltaic plant in Semnan city. They reported system efficiency of about 83%. Nezhad [26] investigated energy storage systems in hybrid cycles. There are other researches in the field of solar energy use and thermoeconomic and environmental studies [27-31].

According to previous studies on the use of biomass fuels and the effect of this type of fuel on reducing greenhouse gas emissions, in the present study of the combined cycle, a Rankine organic cycle with a gas turbine cycle has been proposed. According to the review by the authors, such a cycle has not been investigated so far. Biogas has been used in the gas turbine cycle. The Rankine cycle is considered basic and modified form. The effect of adding a thermal photovoltaic panel before the combustion chamber on the performance of the proposed cycle is also investigated. The effect of ambient temperature, inlet air temperature on the photovoltaic system, inlet air temperature of the turbine, condenser pressure, steam turbine inlet pressure, photovoltaic area and solar radiation intensity on the energy and exergy efficiency of the Rankine-gas turbine hybrid cycle has been investigated.

2. Materials and Methods

2.1. Thermodynamic modelling

The schematic of the proposed power generation system is shown in the Figure 1. Figure 1 (a) shows a simple organic Rankine cycle with a thermal

photovoltaic panel and a gas turbine assembly. Figure 1 (b) shows a modified state of this cycle. It should be noted that the organic Rankine cycle with internal heat exchanger and an open feed organic heater is presented as a modified cycle.

a)

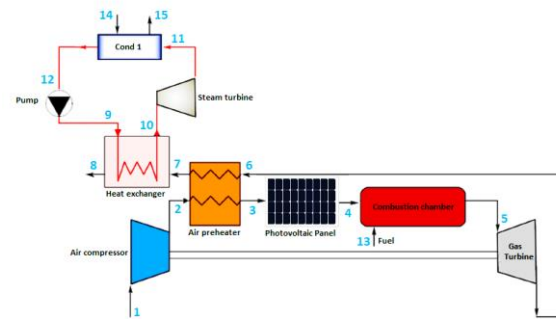

b)

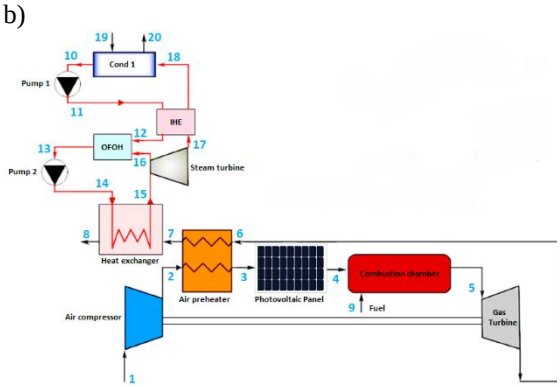

Figure1. Schematic diagram of the biogas- power generation system: a)Basic system (BORC-PV)and b) Modified system(MORC-PV)

In the GT cycle, the environment air with temperature of 298.15 K and pressure of 1 bar compressed through the air compressor (AC) and then flows into air preheater. Upon gaining some heat from flue gas of the turbine exhaust, the air fed into the combustion chamber and mixes with the injected biogas in this chamber. Then, the flue gas is expanded through the gas turbine to produce electricity and then the hot gases pass through the air preheater. Afterward, the gas is supplied to a heat recovery heat exchanger in order to provide required heating capacity of energy for the bottoming cycle. the ORC with an internal heat exchanger (IHE) and an open feed organic heater (OFOH) is used as a modified version of the basic system. an IHE and OFOH are added to the basic ORC (called modified ORC) in order to enhance the performance of the BORC-PV (Fig. 1(b)).

In the BORC (Fig. 1(a)), waste heat of biogas is delivered to the bottoming cycle and then subcooled refrigerant at the outlet of pump is heated to the saturated vapor by utilizing the waste heat. Then the saturated vapor is expanded through the steam turbine to produce power and liquefied to a saturated state after that in a condenser. Finally, the saturated liquid is boosted to the high pressure by a pump, finishing cycle process of the BORC. To improve the performance of the basic ORC, it is proven that an IHE and an OFOH can be added to the basic system (Fig. 1(b)). Accordingly, a part of steam is extracted from the steam turbine and is fed to OFOH, where it is mixed with the cooled stream from outlet of IHE. As a result, the saturated liquid with intermediate pressure is pumped to the high pressure of the system, completing working process of the MORC.

Hybrid solar modules, still rarely found in the solar solutions market, combine solar thermal collectors and photovoltaic panels in the same area of construction where they're installed. This system, called PV/T (Photovoltaic / Thermal) presents advantages to the use of only PV modules, such as hot water cogeneration and saving in installation space and cooling of the PV panels, improving their efficiency. However, flat-plate PV/T collectors absorb radiation less efficiently than conventional flat-plate collectors, may require additional glass coverings to reduce heat loss to the surroundings, have much lower thermal efficiency compared to concentrating collectors, and have higher cost. In this study, a photovoltaic panel is used and the fluid that passes through the channel under the photovoltaic system. This fluid, air, cools the photovoltaic system. A schematic of the photovoltaic panel is shown in Figure 2.

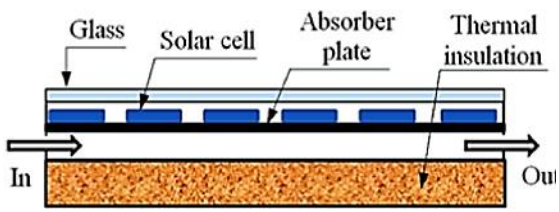

Figure 2. A schematic of Photovoltaic panel with coolant fluid

It is assumed that all components of the cycle operate in steady state conditions. The pressure drop in the combustion chamber and air preheater is considered to be 4% and 5%, respectively. Injectable fuel is applied to the combustion chamber in a combination of 60% methane and 40% carbon dioxide. Air composition also contains 77.48% nitrogen, 20.59% oxygen, 0.03% carbon dioxide and 1.9% water vapor. For each component of the cycle, the equations for

mass and energy conservation equations are written [32,33]:

$$\sum_i \dot{m}_{in} = \sum_o \dot{m}_{out} \quad (1)$$

$$\dot{Q}_{c.v} - \dot{W}_{c.v} = \sum (\dot{m}h)_{out} - \sum (\dot{m}h)_{in} \quad (2)$$

Where $\dot{Q}_{c.v}, \dot{W}_{c.v}, h, out\ and\ in$ are heat and work of control volume, enthalpy, outlet and inlet, respectively. The exergy of each component, $\dot{E}x_{component}$, is calculated as follows[32,33].

$$\dot{E}x_{component} = \dot{m}(h - h_0 - T_0(s - s_0)) + \sum y_i\, ex_{ch,0} + RT_0 \sum y_i\, ln y_i \quad (3)$$

Where $\dot{m}, h, T, s, R, ex_{ch}\ and\ y_i$ are mass flow rate, enthalpy, temperature, entropy, universal gases constant, standard chemical exergy for each compound and mass fraction, respectively. Indices of 0 is dead state. Exergy destruction, $\dot{E}x_{dest}$, and exergy efficiency , η_{ex} are calculated from the following equations[4]:

$$\dot{E}x_{dest} = \sum \dot{E}x_{in} - \sum \dot{E}x_{out} \quad (4)$$

$$\eta_{ex} = \frac{\dot{E}x_{out}}{\dot{E}x_{in}} \quad (5)$$

The exergy destruction ratio, $y_{D,k}$, is defined as the ratio of the exergy destruction of the k[th] element, $\dot{E}x_{dest,k}$, to the total exergy destruction of the system, $\dot{E}x_{dest,tot}$[21,22]

$$y_{D,k} = \frac{\dot{E}x_{dest,k}}{\dot{E}x_{dest,tot}} \quad (6)$$

The relationships of the energy balance and exergy equations for the components of each cycle are derived based on the relations presented above. The obtained equations are summarized in Tables1 and 2.

Table1 Equations for BORC-PV[32,33]

component	Energy balance equation	Exergy balance equation
compressor	$\dot{W}_{AC} = \dot{m}_1(h_2 - h_1)$ $\eta_{is,AC} = \frac{h_1 - h_{2s}}{h_1 - h_2}$	$\dot{E}x_{dest,AC} = \dot{W}_{AC} - (\dot{E}x_2 - \dot{E}x_1)$ $\eta_{ex,AC} = \frac{(\dot{E}x_2 - \dot{E}x_1)}{\dot{W}_{AC}}$
Air preheater	$\eta_{AP} = \frac{\dot{m}_2(h_3 - h_2)}{\dot{m}_6(h_6 - h_7)}$	$\dot{E}x_{dest,AP} = (\dot{E}x_6 - \dot{E}x_7) - (\dot{E}x_3 - \dot{E}x_2)$ $\eta_{ex,AP} = \frac{(\dot{E}x_3 - \dot{E}x_2)}{(\dot{E}x_6 - \dot{E}x_7)}$
PV/T	$\eta_{th,PV} = \frac{\dot{m}_3 c_f (T_4 - T_3)}{A_{PV} G_{irr}}$ $\dot{E}_{PVT} = \tau \times G_{irr} \times \alpha \times r \times A_{PV} \times \eta_r \times (1 - 0.0045(T_{PV} - T_r))$ $\eta_{el,PV} = \frac{\dot{E}_{PVT}}{A_{PV} G_{irr}}$	$\dot{E}x_{dest,PV} = (\dot{E}x_{sun}) - (\dot{E}x_{el,PV} + \dot{E}x_{th,PV})$ $\eta_{ex,PV} = \frac{(\dot{E}x_{el,PV} + \dot{E}x_{th,PV})}{(\dot{E}x_{sun})}$
Combustion chamber	$\dot{Q}_{cc} = \dot{m}_{fuel} \dot{E}x_{ch,fuel}$	$\dot{E}x_{dest,cc} = (\dot{E}x_4 + \dot{E}x_{fuel}) - \dot{E}x_5$ $\eta_{ex,CC} = \frac{(\dot{E}x_5)}{(\dot{E}x_4 + \dot{E}x_{fuel})}$
Gas turbine	$\dot{W}_{GT} = \dot{m}_5(h_5 - h_6)$ $\eta_{is,GT} = \frac{h_5 - h_6}{h_5 - h_{6s}}$	$\dot{E}x_{dest,GT} = (\dot{E}x_5 - \dot{E}x_6) - \dot{W}_{GT}$ $\eta_{ex,CC} = \frac{(\dot{W}_{GT})}{(\dot{E}x_5 - \dot{E}x_6)}$
Heat exchanger	$\dot{Q}_{HX} = \dot{m}_{10}(h_{10} - h_9)$	$\dot{E}x_{dest,HX} = (\dot{E}x_7 - \dot{E}x_8) - (\dot{E}x_{10} - \dot{E}x_9)$ $\eta_{ex,HX} = \frac{(\dot{E}x_{10} - \dot{E}x_9)}{(\dot{E}x_7 - \dot{E}x_8)}$
Steam turbine	$\dot{W}_{ST} = \dot{m}_{10}(h_{11} - h_{10})$ $\eta_{is,ST} = \frac{h_{10} - h_{11s}}{h_{10} - h_{11}}$	$\dot{E}x_{dest,ST} = (\dot{E}x_{10} - \dot{E}x_{11}) - \dot{W}_{ST}$ $\eta_{ex,ST} = \frac{\dot{W}_{ST}}{(\dot{E}x_{10} - \dot{E}x_{11})}$
condenser	$\dot{Q}_{CO} = \dot{m}_{11}(h_{11} - h_{12})$	$\dot{E}x_{dest,CO} = (\dot{E}x_{11} - \dot{E}x_{12}) - (\dot{E}x_{15} - \dot{E}x_{14})$ $\eta_{ex,CO} = \frac{(\dot{E}x_{15} - \dot{E}x_{14})}{(\dot{E}x_{11} - \dot{E}x_{12})}$

Pump	$\dot{W}_{PU} = \dot{m}_9(h_9 - h_{12})$ $\eta_{is,PU} = \frac{h_{12} - h_{9s}}{h_{12} - h_9}$	$\dot{E}x_{dest,PU} = \dot{W}_{PU} - (\dot{E}x_9 - \dot{E}x_{12})$ $\eta_{ex,PU} = \frac{(\dot{E}x_9 - \dot{E}x_{12})}{\dot{W}_{PU}}$
ORC	$\dot{W}_{net,BORC-PV} = \dot{W}_{GT} + \dot{W}_{ST} - \dot{W}_{PU} - \dot{W}_{AC}$	$\dot{E}x_{dest,BORC-PV} = (\dot{E}x_1 + \dot{W}_{PU} + \dot{E}x_{fuel} + \dot{E}x_{14} + \dot{W}_{AC} + \dot{E}x_{sun}) - (\dot{W}_{GT} + \dot{W}_{ST} + \dot{E}x_8 + \dot{E}x_{15} + \dot{E}x_{el,PV})$

Table2 Equations for MORC-PV[32,33]

component	Energy balance equation	Exergy balance equation
Compressor	$\dot{W}_{AC} = \dot{m}_1(h_2 - h_1)$ $\eta_{is,AC} = \frac{h_1 - h_{2s}}{h_1 - h_2}$	$\dot{E}x_{dest,AC} = \dot{W}_{AC} - (\dot{E}x_2 - \dot{E}x_1)$ $\eta_{ex,AC} = \frac{(\dot{E}x_2 - \dot{E}x_1)}{\dot{W}_{AC}}$
Air preheater	$\eta_{AP} = \frac{\dot{m}_2(h_3 - h_2)}{\dot{m}_6(h_6 - h_7)}$	$\dot{E}x_{dest,AP} = (\dot{E}x_6 - \dot{E}x_7) - (\dot{E}x_3 - \dot{E}x_2)$ $\eta_{ex,AP} = \frac{(\dot{E}x_3 - \dot{E}x_2)}{(\dot{E}x_6 - \dot{E}x_7)}$
PV/T	$\eta_{th,PV} = \frac{\dot{m}_3 c_f (T_4 - T_3)}{A_{PV} G_{irr}}$ $\dot{E}_{PVT} = \tau \times G_{irr} \times \alpha \times r \times A_{PV} \times \eta_r \times \left(1 - 0.0045(T_{PV} - T_r)\right)$ $\eta_{el,PV} = \frac{\dot{E}_{PVT}}{A_{PV} G_{irr}}$	$\dot{E}x_{dest,PV} = (\dot{E}x_{sun}) - (\dot{E}x_{el,PV} + \dot{E}x_{th,PV})$ $\eta_{ex,PV} = \frac{(\dot{E}x_{el,PV} + \dot{E}x_{th,PV})}{(\dot{E}x_{sun})}$
Combustion chamber	$\dot{Q}_{cc} = \dot{m}_{fuel} \dot{E}x_{ch,fuel}$	$\dot{E}x_{dest,cc} = (\dot{E}x_4 + \dot{E}x_{fuel}) - \dot{E}x_5$ $\eta_{ex,CC} = \frac{(\dot{E}x_5)}{(\dot{E}x_4 + \dot{E}x_{fuel})}$
Gas turbine	$\dot{W}_{GT} = \dot{m}_5(h_5 - h_6)$ $\eta_{is,GT} = \frac{h_5 - h_6}{h_5 - h_{6s}}$	$\dot{E}x_{dest,GT} = (\dot{E}x_5 - \dot{E}x_6) - \dot{W}_{GT}$ $\eta_{ex,CC} = \frac{(\dot{W}_{GT})}{(\dot{E}x_5 - \dot{E}x_6)}$
Heat exchanger	$\dot{Q}_{HX} = \dot{m}_{15}(h_{15} - h_{14})$	$\dot{E}x_{dest,HX} = (\dot{E}x_7 - \dot{E}x_{14}) - (\dot{E}x_{15} - \dot{E}x_8)$ $\eta_{ex,HX} = \frac{(\dot{E}x_{15} - \dot{E}x_8)}{(\dot{E}x_7 - \dot{E}x_{14})}$
Steam turbine	$\dot{W}_{ST} = \dot{m}_{15}((1-y)(h_{15} - h_{14}) + y(h_{15} - h_{17}))$ $\eta_{is,ST} = \frac{h_{15} - h_{16}}{h_{15} - h_{16s}}$	$\dot{E}x_{dest,ST} = \dot{W}_{ST} - \dot{E}x_{15}$ $\eta_{ex,ST} = \frac{\dot{W}_{ST} - \dot{E}x_{16} - \dot{E}x_{17}}{\dot{E}x_{15}}$
condenser	$\dot{Q}_{CO} = \dot{m}_{19}(h_{20} - h_{19})$	$\dot{E}x_{dest,CO} = (\dot{E}x_{18} + \dot{E}x_{19}) - (\dot{E}x_{20} + \dot{E}x_{10})$ $\eta_{ex,CO} = \frac{(\dot{E}x_{20} + \dot{E}x_{10})}{(\dot{E}x_{18} + \dot{E}x_{19})}$
Pump1	$\dot{W}_{PU1} = \dot{m}_{11}(h_{11} - h_{10})$ $\eta_{is,PU1} = \frac{h_{10} - h_{11s}}{h_{10} - h_{11}}$	$\dot{E}x_{dest,PU1} = \dot{W}_{PU1} - (\dot{E}x_{11} - \dot{E}x_{10})$ $\eta_{ex,PU1} = \frac{(\dot{E}x_{11} - \dot{E}x_{10})}{\dot{W}_{PU1}}$
Pump2	$\dot{W}_{PU2} = \dot{m}_{14}(h_{14} - h_{13})$ $\eta_{is,PU2} = \frac{h_{13} - h_{14s}}{h_{13} - h_{14}}$	$\dot{E}x_{dest,PU2} = \dot{W}_{PU2} - (\dot{E}x_{14} - \dot{E}x_{13})$ $\eta_{ex,PU2} = \frac{(\dot{E}x_{14} - \dot{E}x_{13})}{\dot{W}_{PU2}}$
Internal heat exchanger	$\dot{Q}_{IHE} = \dot{m}_{18}(h_{18} - h_{11})$	$\dot{E}x_{dest,IHE} = (\dot{E}x_{17} - \dot{E}x_{18}) - (\dot{E}x_{12} - \dot{E}x_{11})$ $\eta_{ex,IHE} = \frac{(\dot{E}x_{12} - \dot{E}x_{11})}{(\dot{E}x_{17} - \dot{E}x_{18})}$
Open feed water	$(h_{13} - h_{12}) = y(h_{16} - h_{12})$	$\dot{E}x_{dest,OFOH} = (\dot{E}x_{16} + \dot{E}x_{12}) - \dot{E}x_{13}$ $\eta_{ex,OFOH} = \frac{\dot{E}x_{13}}{(\dot{E}x_{16} + \dot{E}x_{12})}$
ORC	$\dot{W}_{net,MORC-PV} = \dot{W}_{GT} + \dot{W}_{ST} - \dot{W}_{PU1} - \dot{W}_{PU2} - \dot{W}_{AC}$	$\dot{E}x_{dest,BORC-PV} = \sum \dot{E}x_{D,k}$

2.2Exergy-economic modelling

Exergy-economic analysis takes into account both economic and thermodynamic aspects. The equations

for the total capital rate for each component, the return on investment factor are as follows [22]:

$$\dot{Z}_k = \frac{CRF \times \varphi_r \times Z_k}{N} \quad (7)$$

$$CRF = \frac{k_i(1+k_i)^{n_r}}{(1+k_i)^{n_r}-1} \quad (8)$$

In the above relationships, $\varphi_r$is the maintenance factor, $K_i$is the annual interest rate, $n_r$is the system life, and *N* is the total operating hours of the system. The cost balance equations for each component of the system are as follows [21]:

$$c_i \dot{E}x_{i,k} + \dot{Z}_k = c_o \dot{E}x_{o,k} \quad (9)$$

The cost of exergy destruction rate for each component of the system is estimated from the following equation [21]:

$$\dot{C}_{D,k} = c_i \dot{E}x_{dest,k} \quad (10)$$

The difference between the relative cost and the economic exergy factor for each component is derived from the following equations [22]:

$$r_k = \frac{c_{O,k} - c_{i,k}}{c_{i,k}} \quad (11)$$

$$f_k = \frac{\dot{Z}_k}{\dot{Z}_k + \dot{C}_{D,k}} \quad (12)$$

2.3 Evaluate the overall performance of the system

The energy efficiency or thermal efficiency of the proposed simple organic Rankine-gas turbine cycle with the thermal photovoltaic panel is defined as follows [22]:

$$\eta_{th,BORC-PV} = \frac{\dot{W}_{net,BORC-PV}}{\dot{Q}_{cc}} \quad (13)$$

The thermal efficiency of the proposed modified organic Rankine cycle with gas turbine assembly and thermal photovoltaic panel [22]:

$$\eta_{th,MORC-PV} = \frac{\dot{W}_{net,MORC-PV}}{\dot{Q}_{cc}} \quad (14)$$

The exergy efficiency of the proposed BORC with thermal photovoltaic panel is also derived from the following equation:

$$\eta_{ex,BORC-PV} = \frac{\dot{W}_{net,BORC-PV} + \dot{E}x_{el,PV}}{\dot{E}x_{fuel} + \dot{E}x_{sun}} \quad (15)$$

Similarly, for the MORC with PV, the exergy efficiency can be expressed as follows:

$$\eta_{ex,MORC-PV} = \frac{\dot{W}_{net,MORC-PV} + \dot{E}x_{el,PV}}{\dot{E}x_{fuel} + \dot{E}x_{sun}} \quad (16)$$

3.Results and discussion

In this study, the thermodynamic results obtained from the simulation of the proposed cycles in EES software are analysed and then the effects of different cycle parameters on the overall performance of the system are studied. The results of the present study are compared with the reference [20] and the results are shown in Table 3. For this case, isotropic efficiency of compressor, compressor pressure ratio, isotropic efficiency of gas turbine, inlet temperature to combustion chamber, inlet temperature to gas turbine, inlet steam pressure to steam turbine, condenser pressure, inlet temperature difference to heat exchanger, intermediate pressure, isentropic efficiency of steam turbine , isentropic efficiency of the pump, temperature and pressure in the dead state [21]are 86%, 10,86%, 700K, 1250K, 3000kPa, 100kPa, 30K,1062kPa, 85%, 90%, 293.2K and 101.3kPa, respectively. The highest percentage difference between the results of the two studies is less than 5%. The results indicate the good accuracy of modelling presented in the present study. The characteristics of the photovoltaic panel are considered in accordance with Table 4.

Table 5 shows the thermodynamic parameters for both proposed cycles for the case where the photovoltaic panel is used. It can be seen that the modified organic Rankine cycle (MORC-PV) increases the output power by almost 28% compared to the simple organic Rankine cycle or BORC-PV. It can also be seen that the thermal and exergy efficiency has been increased for the modified MORC cycle and the use of photovoltaic panel has been able to significantly increase the output power, energy efficiency and exergy of the cycle. Of course, there is another advantage to using a photovoltaic system, which is the direct generation of electricity. Also, the air passing through the photovoltaic system takes some heat from this system and causes it to cool

down. As the photovoltaic system cools, its electrical efficiency increases.

Table3 Comparison between the results of the present study and the reference [20]

	Present study	[20]
$W_{GT}(kW)$	2373	2444
$W_{st}(kW)$	321.5	321
$W_{AC}(kW)$	1417	1444
$\eta_{th}(\%)$	39.95	39.9
$\eta_{ex}(\%)$	39.3	37.2

Table 4. Characteristics of photovoltaic panels[20]

Parameter	value
Photovoltaic panel area (A_{PV})	0.5562 (m^2)
Solar radiation intensity (G_{irr})	800 (W/m^2)
Mass flow factor (F_R)	0.88
Glass transmittance coefficient (τ)	0.92
Absorption coefficient (α)	0.9
Solar temperature (T_{sun})	5505 (K)
Reference temperature (T_r)	293.15 (K)
reference electrical efficiency (η_r)	0.15
Compact coefficient (r)	0.35
Reference temperature coefficient (β_r)	0.0045

Table5. Comparison of output parameters of cycles

parameters	BORC	BORC-PV	MORC	MORC-PV
$\dot{W}_{GT}(kW)$	2373	2703	2373	2617
$\dot{W}_{ST}(kW)$	321.5	321.5	591	920.7
$\dot{W}_{PU}(kW)$	13.66	13.66	40.59	81.18
$\dot{W}_{AC}(kW)$	1417	1417	1417	1417
$\dot{W}_{net}(kW)$	1264	1594	1466	2040
$\eta_{th}(\%)$	39.5	53.15	46.33	66.47
$\eta_{ex}(\%)$	39.3	48.46	45.58	59.64

Tables 6&7 show the economic exergy parameters for the components of the proposed BORC-PV cycle. The results show that the most exergy degradation occurs in the combustion chamber, which accounts for 53% of the total destruction of the complex. Fuel consumption is in these components. On the other hand, it is clear that among all the components, the highest investment cost is related to the steam turbine. The lowest cost of exergy destruction in this cycle is related to the pump.

Table 6. Values of exergy and exergy-economic parameters obtained from BORC-PV cycle analysis

component	$\dot{E}x_{dest}$(kW)	$\eta_{ex}(\%)$	$y_D(\%)$
Air compressor	95.67	93.25	5.705
Air preheater	101.7	69.9	6.064
photovoltaic	160.7	61.13	9.58
Combustion chamber	793.8	83.69	47.33
Gas turbine	90.98	96.74	5.425
Heat exchanger	353.6	53.32	21.09
Steam turbine	48.71	86.84	2.904
condenser	35.4	22.97	2.111
Pump	1.469	89.25	0.0876
Total	1677	48.46	-

Table 7 Exergy-economic parameters obtained from BORC-PV cycle analysis

Component	$\dot{C}_D$($/h)	$\dot{Z}_k$($/h)	$f_k(\%)$
Air compressor	5.023	1.95	27.97
Air preheater	5.437	0.8735	13.84
Photovoltaic	8.965	0.00335	0.0374
Combustion chamber	44.3	0.066	0.1496
Gas turbine	3.503	0.8076	18.74
Heat exchanger	16	0.062	0.3855

Steam turbine	4.138	3.629	46.72
Condenser	3.798	0.1128	2.885
Pump	0.146	0.24	62.27
Total	91.31	7.633	7.715

Tables 8&9 show the exergy and economic exergy parameters for the MORC-PV combined cycle. In this proposed cycle, it is also clear that the highest exergy degradation occurs due to the irreversibility of the combustion process in the combustion chamber, so that 54% of the total exergy degradation is this component. In this cycle, the steam turbine requires the highest investment cost. Minimal cost and exergy degradation also occur in pump 2.

Table 8. Values of exergy and exergy-economic parameters obtained from MORC-PV cycle

component	$\dot{E}x_{dest}$(kW)	η_{ex}(%)	y_D(%)
compressor	95.67	93.25	4.583
Air heater	101.7	69.9	4.872
Thermal photovoltaic panel	225.5	45.44	10.8
Combustion chamber	834.3	82.76	39.97
Gas turbine	110.2	95.96	5.279
Heat exchanger	174.2	66.54	8.344
Steam turbine	163.8	88.08	20.02
condenser	20.29	33.22	0.9718
Pump1	34.51	92.27	0.01653
Pump2	16.65	92.21	0.7976
Open feed-organic heater	55.1	75.79	2.639
Internal heat exchanger	1.473	69.01	0.07
total	1833	59.64	98.14

Table 9. Values of exergy-economic parameters obtained from MORC-PV cycle

component	$\dot{C}_D$($/h)	$\dot{Z}_k$($/h)	f_k(%)
compressor	5.023	1.95	27.97
Air heater	5.437	0.8735	13.84
Thermal photovoltaic panel	12.58	0.00335	0.0266
Combustion chamber	37.75	0.0655	0.1732
Gas turbine	4.242	0.0155	0.3651
Heat exchanger	17.64	0.0926	0.5221
Steam turbine	13.92	8.934	17.59
condenser	1.548	0.2647	14.6
Pump1	0.043	0.1039	70.51
Pump2	0.162	0.3604	69.01
Open feed-organic heater	4.205	0	0
Internal heat exchanger	0.112	0.075	40.17
total	102.7	11.38	9.982

In this section, the effects of several important thermodynamic parameters on the overall performance of the proposed BORC and MORC cycles are studied. Parameters such as ambient temperature, inlet temperature to photovoltaic panel, inlet temperature to gas turbine, condenser pressure, steam turbine, inlet pressure, photovoltaic panel area and solar radiation per unit area of photovoltaic panel are among the studied parameters.

Figure 3 shows the effect of ambient temperature on the energy and exergy efficiencies of the two proposed cycles BORC-PV and MORC-PV. With increasing ambient temperature, energy efficiency and exergy efficiency improve in both cycles, although this improvement is slightly greater in the MORC cycle than in the BORC.

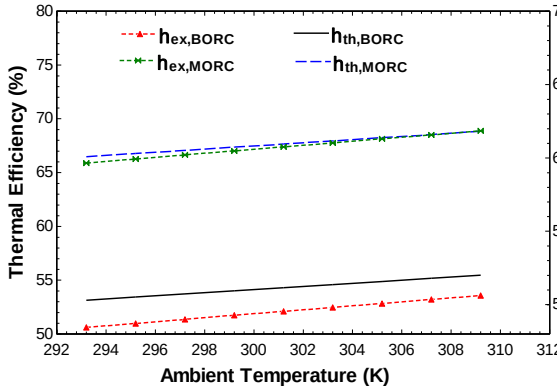

Figure 3. The effect of ambient temperature on the thermal and exergy efficiency of BORC and MORC cycles

Figure 4 shows the effect of increasing the inlet air temperature to the thermal photovoltaic panel on the thermodynamic performance of BORC-PV and MORC-PV cycles. It is found that with increasing the temperature of the inlet air to the thermal photovoltaic panel, the exergy and thermal efficiencies increase.

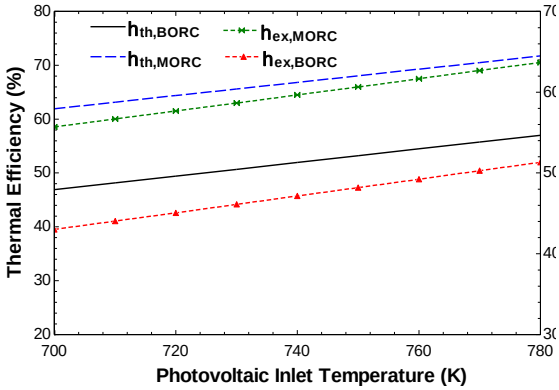

Figure 4. Thermal and exergy efficiency changes of BORC and MORC cycles according to inlet temperature of photovoltaic panel

Figure 5 shows the effects of increasing the turbine inlet temperature on the thermal efficiency and exergy of the proposed BORC-PV and MORC-PV cycles. It is known that with increasing the temperature of the inlet air to the thermal photovoltaic panel, the exergy and thermal efficiencies increase. The reason for this increase is that as the inlet temperature to the photovoltaic panel increases, the inlet temperature to the combustion chamber also increases, thus increasing the thermal and exergy efficiency in both cycles.

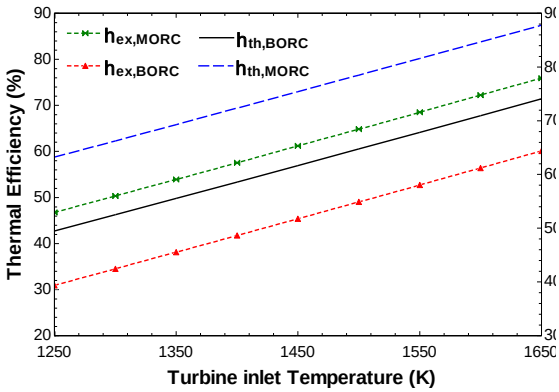

Figure 5. The effect of turbine inlet temperature on the thermal and exergy efficiency of the proposed BORC and MORC cycles

Figure 6 shows the effects of condenser pressure change on the energy efficiency and exergy of the proposed BORC-PV and MORC-PV cycles. The reason for this behaviour is that as the condenser pressure decreases, the output power of the steam turbine in the cycle is affected and reduced. This negative effect on the thermal and exergy efficiencies of the BORC-PV cycle is also much higher.

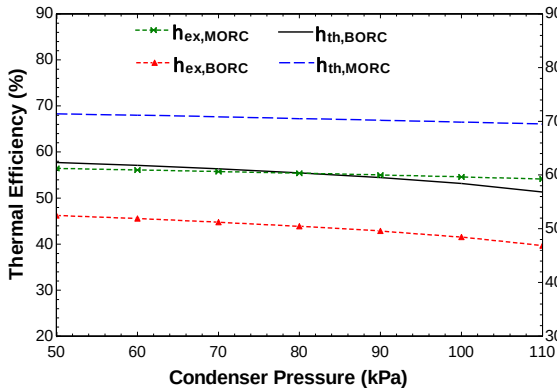

Figure 6. Effect of condenser pressure changes on exergy and thermal efficiency of BORC and MORC cycles

Figure 7 illustrates the effects of changing the steam turbine inlet pressure on the energy and exergy efficiencies of the two modified BORC-PV and MORC-PV cycles. It is known that by increasing the steam turbine inlet pressure, it has a negative effect on the energy and exergy efficiencies of both cycles. The maximum efficiency occurs at a working pressure of 2000 kPa for both cycles. The effect of a 50% increase in steam turbine inlet pressure results in a nearly 20% reduction in the MORC-PV improved exergy cycle efficiency.

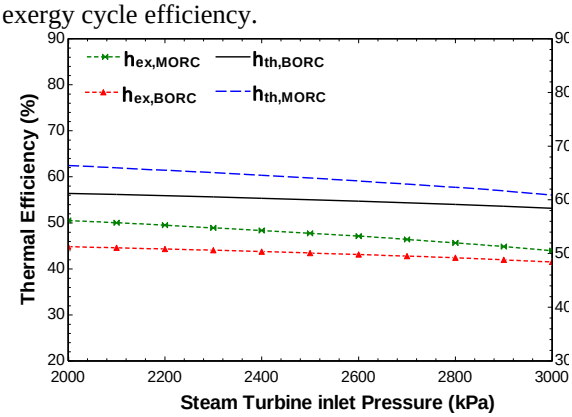

Figure7. Steam turbine inlet pressure changes on exergy and thermal efficiency of BORC and MORC cycles

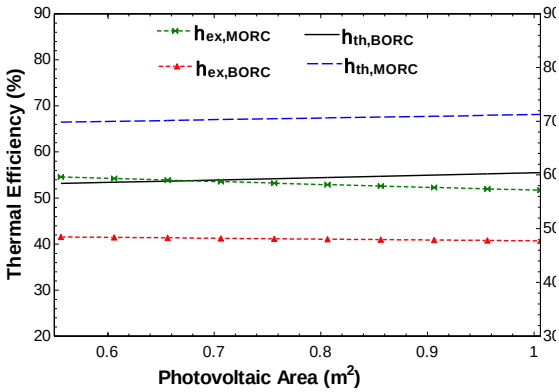

Figure 8. Effect of changes in photovoltaic panel surface on exergy and thermal efficiency of BORC and MORC cycles

Figure 8 displays the effects of changing the surface area of a thermal photovoltaic panel on the energy efficiency and exergy of both the BORC-PV and MORC-PV cycles. The results show that increasing the surface of photovoltaic panel improves not only the thermal efficiencies of photovoltaic system but also the energy efficiency of both cycles, but this increase in surface area has an adverse effect on the exergy and electrical efficiency of photovoltaic panels.

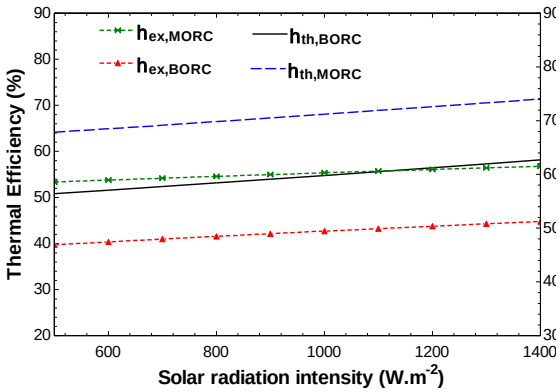

Figure 9. Effect of changes in solar radiation intensity on exergy and thermal efficiency of BORC and MORC cycles

Figure 9 shows the effects of increasing the intensity of solar radiation per unit area of the PV panel on the energy and exergy efficiencies of the two proposed cycles. It is observed that with increasing intensity of sunlight, thermal and exergy efficiencies improve. The reason for this thermal behaviour is that as the intensity of radiation per unit area of photovoltaic thermal panels increases, the thermal and electrical efficiency of these panels increases, and this directly affects the overall performance of both sets.

4.Conclusion

In this study, a combined Rankine organic cycle with gas turbine cycle was studied by applying modifications such as adding a thermal photovoltaic panel with air-fluid before the gas turbine combustion chamber in both simple and improved modes. The modelling results of the two proposed cycles showed that for the improved MORC-PV cycle, the output power can be improved up to 28% compared to the basic state. The exergy and thermal efficiencies increased by 23 and 25% for the improved MORC cycle, respectively. Also, the results of parametric studies showed that the inlet temperature of the photovoltaic panel, ambient temperature, inlet temperature of the gas turbine and the intensity of solar radiation have a positive effect on the overall performance of both cycles.

However, increasing condenser pressure and steam turbine inlet pressure had a negative effect on the performance of both proposed circuits. Studies show that in both cycles the combustion chamber, as the largest exergy destroyer, in some cases destroys more than half of the system's exergy. In contrast, the pump can be described as the least destructive exergy in both cycles.

On the other hand, observing the results, it can be seen that the lowest exergy efficiency is related to the condenser in both systems, while the gas turbine with the highest exergy efficiency is well placed in both systems. The reason for this behaviour is the use of thermal photovoltaic panel. It precedes the Brayton combustion chamber and naturally decreases with increasing inlet temperature to the combustion chamber. Therefore, it reduces the exergy degradation in the combustion chamber and also improves the inlet temperature to the gas turbine.

Nomenclature

$\dot{Q}$	Heat(kW)
$\dot{w}$	Power(kW)
$\dot{E}x$	Exergy(kW)
K_i	the annual interest rate
$\dot{Z}$	investment cost rate of components ($ yr $^{-1}$)
f	exergoeconomic factor
$\dot{m}$	mass flow rate(kg/s)
n_r	the system life

r_k	relative cost difference
$y_{D,k}$	exergy destruction ratio
A	Area(m^2)
G	Solar radiation(W/m^{-2})
h	Enthalpy(kJ/kg)
P	Pressure(kPa)
T	Temperature(K)
y	mass fraction
N	the total operating hours of the system
R	universal gases constant
Z	investment cost of components ($)
ex	Specific exergy(kJ/kg)
s	Entropy(kJ/kg.K)

Greek symbols

φ_r	maintenance factor
τ	Transmittance coefficient
α	Absorptivity coefficient
η	Efficiency(%)

Subscripts and superscripts

0	Dead state
AC	air compressor
AP	air preheater
BORC	basic ORC
c.v	Control volume
cc	combustion chamber
ch	chemical
CI	capital investment
co	condenser
CRF	capital recovery factor
des	destruction
el	electrical
eva	evaporator
ex	exergy
F	fuel
GT	Gas turbine
HX	heat exchanger
in	inlet
irr	irradiation
is	isentropic
out	outlet
Pu	Pump
PV	photovoltaic
q	Heart transfer
ST	Steam turbine
th	thermal
tot	total
tur	Turbine

References

1. Alhamid, M.I., et al., Potential of geothermal energy for electricity generation in Indonesia: A review. Renewable and Sustainable Energy Reviews, 2016. **53**: p. 733-740.
2. Michaelides, E.E.S., Future directions and cycles for electricity production from geothermal resources. Energy Conversion and Management, 2016. **107**: p. 3-9.
3. Shokati, N., F. Ranjbar, and M. Yari, Exergoeconomic analysis and optimization of basic, dual-pressure and dual-fluid ORCs and Kalina geothermal power plants: A comparative study. Renewable Energy, 2015. **83**: p. 527-542.
4. Kalina, A.I. Combined cycle and waste heat recovery power systems based on a novel thermodynamic energy cycle utilizing low-temperature heat for power generation. in Turbo Expo: Power for Land, Sea, and Air. 1983. American Society of Mechanical Engineers.
5. Balat, M., Potential importance of hydrogen as a future solution to environmental and transportation problems. International journal of hydrogen energy, 2008. **33**(15): p. 4013-4029.
6. Winter, C.-J., Hydrogen energy—Abundant, efficient, clean: A debate over the energy-system-of-change. International Journal of hydrogen energy, 2009. **34**(14): p. S1-S52.
7. Arabul, F.K., et al., Providing energy management of a fuel cell–battery–wind turbine–solar panel hybrid off grid smart home system. International journal of hydrogen energy, 2017. **42**(43): p. 26906-26913.
8. Kang, J.S., et al., Nickel-based tri-reforming catalyst for the production of synthesis gas. Applied Catalysis A: General, 2007. **332**(1): p. 153-158.
9. Braga, L.B., et al., Hydrogen production by biogas steam reforming: A technical, economic and ecological analysis. Renewable and Sustainable Energy Reviews, 2013. **28**: p. 166-173.
10. Ahmadi, P., I. Dincer, and M.A. Rosen, Energy and exergy analyses of hydrogen production via solar-boosted ocean thermal energy conversion and PEM electrolysis.

International Journal of Hydrogen Energy, 2013. **38**(4): p. 1795-1805.
11. Jiang, L., et al., Experimental study on a resorption system for power and refrigeration cogeneration. Energy, 2016. **97**: p. 182-190.
12. Momirlan, M. and T.N. Veziroglu, The properties of hydrogen as fuel tomorrow in sustainable energy system for a cleaner planet. International journal of hydrogen energy, 2005. **30**(7): p. 795-802.
13. Rahmouni, S., et al., A technical, economic and environmental analysis of combining geothermal energy with carbon sequestration for hydrogen production. Energy Procedia, 2014. **50**: p. 263-269.
14. Bicer, Y. and I. Dincer, Development of a new solar and geothermal based combined system for hydrogen production. Solar Energy, 2016. **127**: p. 269-284.
15. Balta, M.T., I. Dincer, and A. Hepbasli, Exergoeconomic analysis of a hybrid copper–chlorine cycle driven by geothermal energy for hydrogen production. International journal of hydrogen energy, 2011. **36**(17): p. 11300-11308.
16. Quoilin, S., et al., Thermo-economic optimization of waste heat recovery Organic Rankine Cycles. Applied thermal engineering, 2011. **31**(14-15): p. 2885-2893.
17. Tiwari, D., et al., Energy and exergy analysis of solar driven recuperated organic Rankine cycle using glazed reverse absorber conventional compound parabolic concentrator (GRACCPC) system. Solar Energy, 2017. **155**: p. 1431-1442.
18. Tchanche, B.F., M. Pétrissans, and G. Papadakis, Heat resources and organic Rankine cycle machines. Renewable and Sustainable Energy Reviews, 2014. **39**: p. 1185-1199.
19. Khaljani, M., R.K. Saray, and K. Bahlouli, Comprehensive analysis of energy, exergy and exergo-economic of cogeneration of heat and power in a combined gas turbine and organic Rankine cycle. Energy Conversion and Management, 2015. **97**: p. 154-165.
20. Astolfi, M., et al., Technical and economical analysis of a solar–geothermal hybrid plant based on an Organic Rankine Cycle. Geothermics, 2011. **40**(1): p. 58-68.
21. Gholizadeh, T., M. Vajdi, and F. Mohammadkhani, Thermodynamic and thermoeconomic analysis of basic and modified power generation systems fueled by biogas. Energy conversion and management, 2019. **181**: p. 463-475.
22. Hezaveh, S.A., S.D. Farahani, and M. Alibeigi, Technical-economic analysis of the organic rankine cycle with different energy sources. Journal of Solar Energy Research, 2020. **5**(1): p. 362-373.
23. Sohbatloo, A. and F.A. Boyaghchi, Cascade organic Rankine cycle using LNG cold energy: Energetic and exergetic assessments. Journal of Solar Energy Research, 2017. **2**(4): p. 329-335.
24. Ouagued, M., Magnesium–Chlorine Cycle for Hydrogen Production Driven by Solar Parabolic Trough Collectors. Journal of Solar Energy Research, 2021. **6**(3): p. 799-813.
25. Gharibshahian, I., S. Sharbati, and A.A. Orouji, The Design and Evaluation of a 100 kW Grid Connected Solar Photovoltaic Power Plant in Semnan City. Journal of Solar Energy Research, 2017. **2**(4): p. 287-293.
26. Aryan Nezhad, M., Frequency Control and Power Balancing in a Hybrid Renewable Energy System (HRES): Effective Tuning of PI Controllers in the Secondary Control Level. Journal of Solar Energy Research, 2022. **7**(1): p. 963-970.
27. Shadi, M., S. Davodabadi Farahani, and A. Hajizadeh Aghdam, Energy, Exergy and Economic Analysis of Solar Air Heaters with Different Roughness Geometries. Journal of Solar Energy Research, 2020. **5**(2): p. 390-399.
28. Farahani, S.D. and R. Gholipour, Dynamic Simulation of Solar Desalination: Investigation of Climatic Conditions and Carbon Dioxide Emissions. Journal of Solar Energy Research, 2020. **5**(3): p. 498-505.
29. Farahani, S.D. and M. Alibeigi, Investigation of power generated from a PVT-TEG system in Iranian cities. Journal of Solar Energy Research, 2020. **5**(4): p. 603-616.
30. Farahani, S.D., M.A. Sarlak, and M. Alibeigi, Thermal analysis of PVT-HEX system: electricity efficiency and air

conditioning system. Journal of Solar Energy Research, 2021. **6**(1): p. 625-633.
31. Farahani, S.D., A.D. Farahani, and P. Oraki, Improving Thermal Performance of Solar Water Heater Using Phase Change Material and Porous Material. Heat Transfer Research, 2021. **52**(16).
32. Bejan, A., G. Tsatsaronis, and M.J. Moran, Thermal design and optimization. 1995: John Wiley & Sons.
33. Szargut, J., D.R. Morris, and F.R. Steward, Exergy analysis of thermal, chemical, and metallurgical processes. 1987.